UDK 669.715.018.8
Original scientific article/Izvirni znanstveni članek

ISSN 1580-2949
MTAEC9, 56(4)407(2022)

STUDY OF THE CORROSION PROCESS OF A PEO-TREATED ALUMINUM ALLOY IN DIFFERENT CONCENTRATIONS OF NaCl

ŠTUDIJ PROCESA KOROZIJE S PEO OBDELANE ALUMINIJEVE ZLITINE Z RAZLIČNO KONCENTRACIJO NaCl

Yuanji Shi[1,2*], Yunzhong Dai[1,4], Guoqiang Gao[2], Cheng Cheng[3], Yunyun Song[1]

[1]Key Laboratory of Modern Agricultural Equipment and Technology, Jiangsu University, Zhenjiang, China
[2]Industrial Perception and Intelligent Manufacturing Equipment Engineering Research Center of Jiangsu Province, Nanjing Vocational University of Industry Technology, Nanjing, China
[3]College of Material Science and Technology, Nanjing University of Aeronautics and Astronautics, Nanjing, China
[4]Department of Modern Manufacturing Engineering, Yibin Vocational and Technical College, Yibin, China

Prejem rokopisa – received: 2022-03-21; sprejem za objavo – accepted for publication: 2022-06-28

doi:10.17222/mit.2022.452

Plasma electrolytic oxidation (PEO) treated ceramic coatings were formed in silicate-based electrolytes without and with the addition of Al_2O_3, on an aluminum alloy. It was found that the coating produced in an electrolyte containing 7 g/L of Al_2O_3 exhibited the most superior corrosion properties. The corrosion properties of the coatings in 0.5 M and 1 M NaCl solutions were studied by means of potentiodynamic polarization and electrochemical impedance spectroscopy (EIS). The results proved that the coating can protect the substrate from the corrosion due to aggressive Cl^- in 0.5 M NaCl after 384-h immersion. However, it cannot protect the substrate after 384-h immersion in 1 M NaCl solution. The potentiodynamic polarization results matched well with the EIS test results.

Keywords: aluminum alloy, plasma electrolytic oxidation, ceramic coatings, electrochemical impedance spectroscopy, corrosion

Avtorji v prispevku opisujejo keramične prevleke izdelane s plazemsko elektrolitsko oksidacijo (PEO). Te so nastale na izbrani aluminijevi (ZL101A) zlitini v silikatnem elektrolitu brez in z dodatkom Al_2O_3. Avtorji so ugotovili, da je prevleka z najboljšo odpornostjo proti koroziji nastala v elektrolitu, ki je vseboval 7 g/l Al_2O_3. Nadalje so študirali korozijske lastnosti izdelanih prevlek s potencio-dinamično polarizacijo in elektrokemijsko impedančno spektroskopijo (EIS) v 0,5 molarni (M) in 1 M raztopini NaCl. Rezultati testov so pokazali, da prevleka lahko zaščiti substrat (Al zlitino) pred korozijsko zelo agresivnimi ioni klora (Cl^-), če je le ta potopljen v 0,5 M raztopino NaCl tudi do 384 ur. Vendar pa ga ne ščiti pred korozijo, če je le-ta potopljen 384 ur v 1 M raztopini NaCl. Rezultati potencio-dinamične polarizacije so se dobro ujemali z rezultati EIS testov.

Ključne besede: aluminijeva zlitina, plazemska elektrolitska oksidacija, keramične prevleke, elektrokemijska impedančna spektroskopija, korozija

1 INTRODUCTION

Aluminum and its alloys are widely used in industrial engineering due to their superior properties, that is, low density, great specific strength and good ductility. Nevertheless, their shortcomings, i.e., low surface hardness and poor corrosion resistance, have extremely limited their wide applications in many industrial fields.[1,2]

In recent years, various surface-modification methods have been proposed to prevent aluminum alloys from corrosion in a severe industrial environment. Among these great techniques, plasma electrolytic oxidation (PEO) seems to be the most favorable surface-treatment method since the year 2000.[3,4] It is a technique used at high voltages to grow an oxide coating on an aluminum alloy surface. During a PEO process, the substrate alloy is the anode, while the gas layer enshrouding the surface of the alloy consists of oxygen. Specifically, when the dielectric gas layer completely covers the anode surface, numerous sparks appear, accompanied by the gas bubbles of the PEO treatment, provided that the applied voltage is constantly higher than the breakdown voltage. Then, a ceramic coating can be formed on the metal surface during the chemical reactions in a plasma environment. The coatings produced with the PEO treatment are of good corrosion resistance.[5–8] Therefore, the PEO method has been popularly used in these years to produce coatings with superior corrosion properties on aluminum alloys.

According to previous researches, it is acknowledged that the PEO treatment is a multifactor-controlled process.[9] The properties of PEO coatings are determined by many influencing factors, such as the substrate material,[10] electrical parameters,[10–13] oxidation time,[14,15] additives[8,16–18] and the main electrolyte composition.[19] Generally, silicate-based electrolytes are the most widely employed electrolytes. However, there are only a few studies of the corrosion of the coatings formed on aluminum alloys with the PEO method. Thus, in this study, we want to comprehensively study the corrosion properties

---

*Corresponding author's e-mail:
yuanji_shi@hotmail.com (Y. J. Shi)

of PEO coatings formed on ZL101A aluminum alloy in silicate-based electrolytes.

In this work, PEO coatings were formed on ZL101A aluminum alloy in silicate-based electrolytes with the addition of Al_2O_3. Then, potentiodynamic polarization and electrochemical impedance spectroscopy (EIS) were carried out to study the long-term immersion corrosion process of the coatings in both 0.5 M and 1 M NaCl solutions. X-ray photoelectron spectroscopy (XPS) was used to study the corrosion products of the coatings after immersion in the NaCl solution.

2 EXPERIMENTAL PART

The material was ZL101A aluminum alloy cut form an Al sheet. Its nominal composition is as follows: Mg (0.45–0.7 *w*/%), Si (6.5–7.5 *w*/%), Zn (0.07 *w*/%), Fe (0.19 *w*/%), Cu (0.05 *w*/%) and balance Al. Cylinder specimens (with a thickness of 3 mm and diameter of 40 mm) were used as the substrate in this study. To ensure their smoothness, the raw specimens were ground with 200, 500, 800, 1200 grit alumina waterproof abrasive paper. After that, they were ultrasonically degreased in ethanol for 20 min, rinsed in distilled water and dried in ambient air.

For the PEO process, a specimen was registered as the anode and a stainless-steel barrel measuring 200 mm in diameter and 400 mm in length was used as the cathode. The specimen was set at the center of the circle in the barrel with the electrolyte. A silicate-based aqueous solution (Na_2SiO_3 (18 g/L) + KOH (3 g/L) + NaF (4 g/L)) was used as the electrolyte. The concentration of additive Al_2O_3 particles (< 20 nm) in the electrolyte solution was varied from 3 g/L to 9 g/L with +2 g/L intervals. PEO coatings were formed under a constant current density of 150 mA/cm^2 over 40 min. Next, the barrel was placed in cold water with a water-cooled system to keep the temperature below 35 °C all the time during the PEO treatment. After this treatment, the PEO-treated samples were rinsed in deionized water and dried in hot air.

Electrochemical experiments were performed in the NaCl aqueous solution (pH of app. 7.0) at room temperature (app. 25 °C) using an electrochemical system (CS350, Wuhan Corrtest, China). Along with the system, a three-electrode cell was used, composed of a weight-saving platinum electrode, a saturated calomel electrode (SCE) and the uncoated or coated specimens. They were used as the auxiliary electrode, reference electrode and working electrode, respectively. The working electrode was made by inlaying pieces of uncoated and coated square samples (about 1 cm^2) into an in-house-made Teflon plate, full of resin. The testing electrolyte used was 0.5 M or 1 M NaCl aqueous solution. Prior to the electrochemical test, the testing specimens were immersed in the NaCl solution for about 30 min to get a stabilized open circuit potential. The potentiodynamic polarization curves of the samples were obtained using an applied scanning rate of 1.0 mV/s and a scanning region of –1.0 V to 0 V with respect to the open circuit potential. CorShow was used to deal with the data of the potentiodynamic polarization test. Electrochemical impedance spectroscopy (EIS) was applied in the potentiostatic mode within a frequency range of 10^5 Hz to 10^{-1} Hz with a perturbation amplitude signal of 10 mV. The specimens were exposed to the NaCl solution for different durations, i.e., (0.5, 24, 48, 96, 192 and 384) h. The EIS plots obtained were analyzed using ZSimpWin3.10. All the tests were repeated at least three times to ensure reproducibility and reliability.

The surface and cross-sectional morphology of the coatings were observed using scanning electron microscopy (SEM, ISM-6510). The thicknesses of the coatings were determined by measuring the cross-sections of the coatings. In addition, X-ray photoelectron spectra (XPS) were obtained with a Thermo Escalab 250Xi photoelectron spectrometer using an AlK_α source with energy of 1486.6 eV. The surfaces of the coatings were etched for 1 min with an argon-ion beam before the XPS analysis to reduce the carbon contamination. Binding energies were corrected relative to the C 1s signal at 284.6 eV. The analysis of the obtained data was processed by the Xpspeak 4.1 software.

To evaluate the effect of the Al_2O_3 concentration on the corrosion resistance of the PEO coatings formed in silicate-based electrolytes, potentiodynamic polarization tests were carried out, identifying the optimum Al_2O_3 concentration for the PEO process. The obtained polarization curves of the PEO coatings are depicted in **Figure 1**. This figure shows that the coating fabricated in the electrolyte with 7 g/L of Al_2O_3 had the lowest corrosion current density (i_{corr}) and highest corrosion potential (E_{corr}) among the five examined Al_2O_3 concentrations. Therefore, further investigations were focused on this concentration.

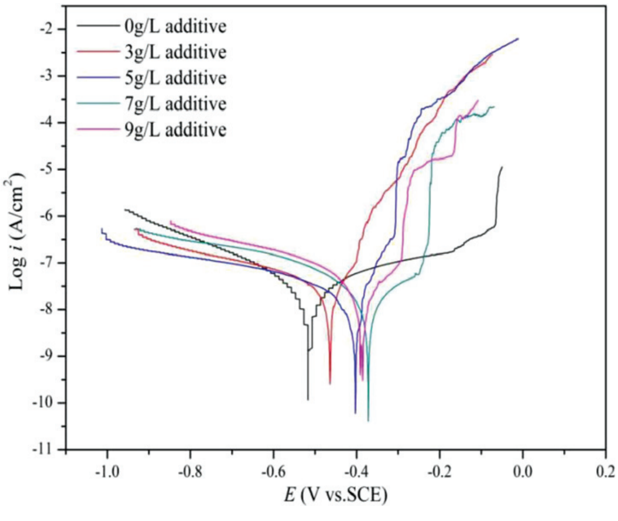

Figure 1: Potentiodynamic polarization curves of the aluminum alloy with PEO coatings formed in electrolytes containing (0, 3, 5, 7 and 9) g/L Al_2O_3 and immersed in 0.5 M NaCl for 0.5 h

3 RESULTS AND DISCUSSION

3.1 Morphology of PEO coatings

Figure 2 shows the surface and cross-sectional morphologies of the PEO coatings formed in the silicate-based electrolyte under the current density of 150 mA/cm^2 for 40 min. The surface morphology of the PEO coating formed in 7 g/L Al_2O_3 containing electrolyte is shown in **Figure 2a**. Numerous discharge channels and regions resulting from the rapid cooling of molten materials are presented on the surface (see **Figure 2a**). At the discharge channel sites, the temperature could suddenly increase to approximately 10^4 K,[20] which was high enough for the coating to melt. The molten alumina flowed out of the channels and the anionic components such as SiO_3^{2-} enter the channels making sharp and distinctly visible boundaries at the same time. And due to the rapidly cooling system, the molten alumina solidified immediately. The above process resulted in a coating with numerous micropores on its surface. The pore size ranged from 1–6 µm. The surface view obtained in this study shows that the coating has a relatively dense structure without considerable cracking. The presence of some pores is expected because of the nature of the PEO process.

The cross-sectional morphologies of the PEO coatings produced in the silicate-based electrolyte with (0, 5 and 9) g/L of Al_2O_3 are shown in **Figures 2b**, **2c** and **2d**. The thickness of the coatings formed in (0, 3, 5, 7 and 9) g/L Al_2O_3 containing electrolytes is approximately (26, 32, 35, 39 and 38) µm, respectively. The link between the coating and the substrate is without any cracking, which indicates good adhesion of the coating to the substrate.

3.2 XPS analysis before corrosion

The effects of additive Al_2O_3 on PEO coatings was estimated on the basis of the chemical state of the surface of the coating. The XPS analysis of the PEO coatings formed in the silicate-based electrolyte without and with the addition of 7 g/L Al_2O_3 is shown in **Figure 3**. This figure presents the Al 2p core level spectra of the PEO coatings formed in the Al_2O_3 free and 7 g/L Al_2O_3 containing electrolytes. The binding energy of Al 2p of the PEO coatings formed in these two electrolytes is 74.28 eV and 74.36 eV, respectively. The difference in the binding energy of the coatings may be owing to the incorperation of additive Al_2O_3. The fact that the Al 2p spin-orbit components of the coating produced in 7 g/L

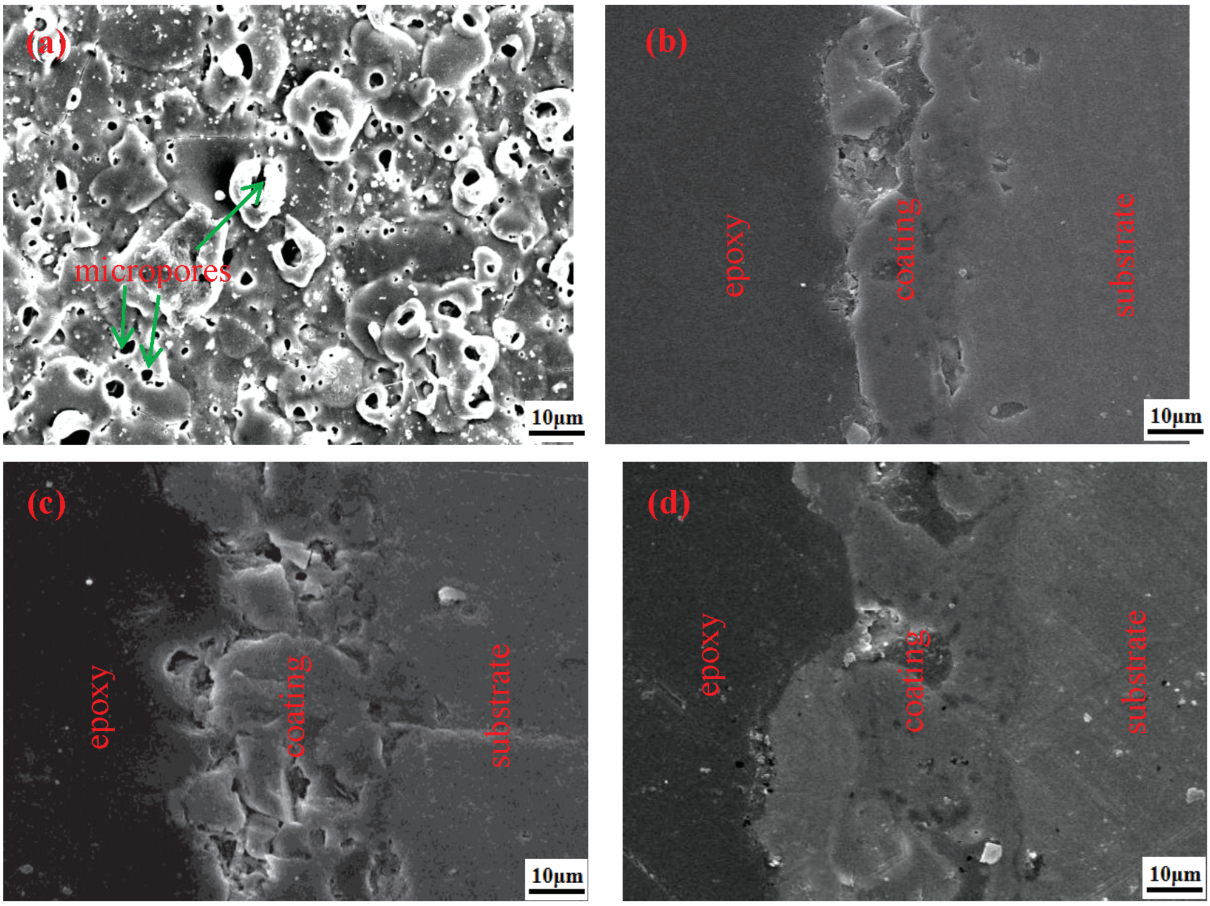

Figure 2: PEO coating morphology: a) surface (7 g/L Al_2O_3 containing electrolyte), b) cross-section (without Al_2O_3), c) cross-section (5 g/L Al_2O_3), d) cross-section (9 g/L Al_2O_3)

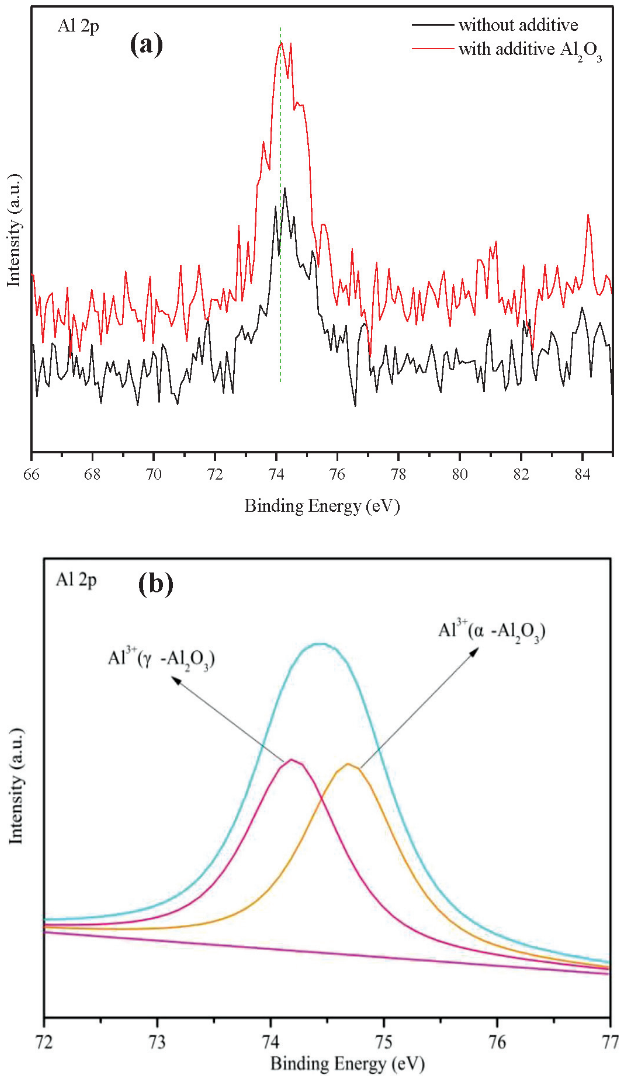

Figure 3: XPS analysis of PEO coatings formed in silicate-based electrolyte without and with the addition of 7 g/L Al_2O_3: a) Al 2p core level, b) high-resolution spectrum of Al 2p corresponding to the PEO coating formed in 7 g/L Al_2O_3 containing electrolyte

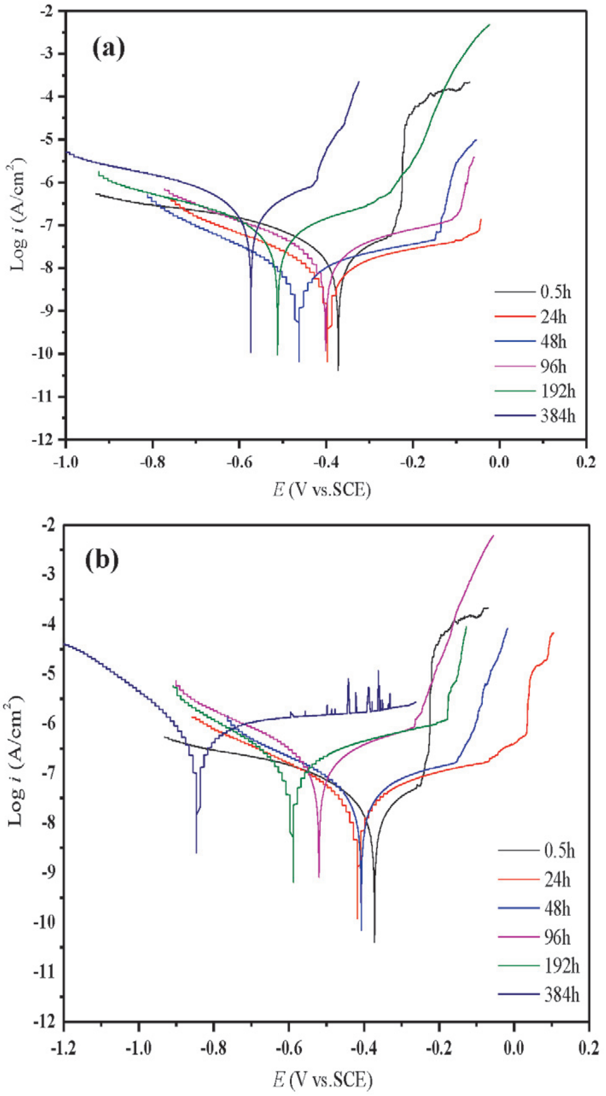

Figure 4: Potentiodynamic polarization curves of PEO-coated aluminum alloy formed in 7 g/L Al_2O_3 containing electrolyte after different immersion times of 0.5–384 h in the solutions: a) 0.5 M NaCl, b) 1 M NaCl

Al_2O_3 containing electrolyte are shifted towards higher binding energy than the coating produced in the Al_2O_3 free electrolyte suggests that some of the additive Al_2O_3 was incorporated into the coating. **Figure 3b** shows the high-resolution spectrum of Al 2p. It is presented that the single Al 2p peak at 74.36 eV, typical for α-Al_2O_3 and γ-Al_2O_3, can be decomposed into two peaks at 74.70 eV and 74.20 eV.

3.3 Corrosion behavior of PEO coatings

3.3.1 Potentiodynamic polarization

The potentiodynamic polarization curves of the PEO-coated specimen formed in 7 g/L Al_2O_3 containing electrolyte after the immersion times of (0.5, 24, 48, 96, 192 and 384) h in 0.5 M and 1 M NaCl aqueous solutions are shown in **Figure 4**. In general, a more noble corrosion potential (E_{corr}) and lower corrosion current density (i_{corr}) represented a lower corrosion rate and good corrosion properties. **Figure 4** shows that the corrosion potential (E_{corr}) first decreased before the immersion for 48 h, then increased after 48 h and decreased again after the immersion for 96 h. Nevertheless, the corresponding corrosion current density (i_{corr}) first increased, then decreased and increased in 0.5 M NaCl aqueous solution. Meanwhile, the same changes occurred to the coating, immersed in 1 M NaCl aqueous solution during the potentiodynamic polarization test. This indicated that the corrosion resistance of the PEO-coated specimen first decreased, then increased and finally decreased in both 0.5 M and 1 M NaCl solutions. Furthermore, in both 0.5 M and 1 M NaCl solutions, the corrosion current density of the PEO coating formed in 7 g/L Al_2O_3 containing electrolyte was lower by about 30 orders than the

PEO coating formed in 0 g/L Al_2O_3 containing electrolyte.

3.3.2 EIS study

3.3.2.1 EIS spectra

To obtain additional information on the properties of the coating as well as on the corrosion process at the metal/electrolyte interface, EIS spectra were recorded during the immersion in 0.5 M and 1 M NaCl aqueous solutions at room temperature for a prolonged duration of up to 384 h. The corrosion behavior of the PEO coating produced in 7 g/L Al_2O_3 containing electrolyte and immersed in the above solutions for (0.5, 24, 48, 96, 192 and 384) h was studied with EIS tests. The EIS spectra (Nyquist plots) for the immersed coating are shown in **Figures 5a** and **5b**. In 0.5 M aqueous NaCl, the radius of the capacitive loop decreased in 0.5–384 h immersion process (see **Figure 5a**). After 384-h immersion, the radius of the loop only became smaller. However, in the 1M NaCl solution, the radius of the loop greatly decreased after 24-h immersion (see **Figure 5b**). After 384 h, an inductive loop appeared. In both 0.5 M and 1 M NaCl aqueous solution, the radius of the loop changed homogeneously. That is, in 0.5 M NaCl aqueous solution, the radius of the loop decreased before the immersion time of 48 h, then increased after 48 h and again decreased after 96 h; in 1 M NaCl, the radius of the capacitive loop decreased before the immersion time of 24 h, then increased after 24 h and again decreased after 48 h.

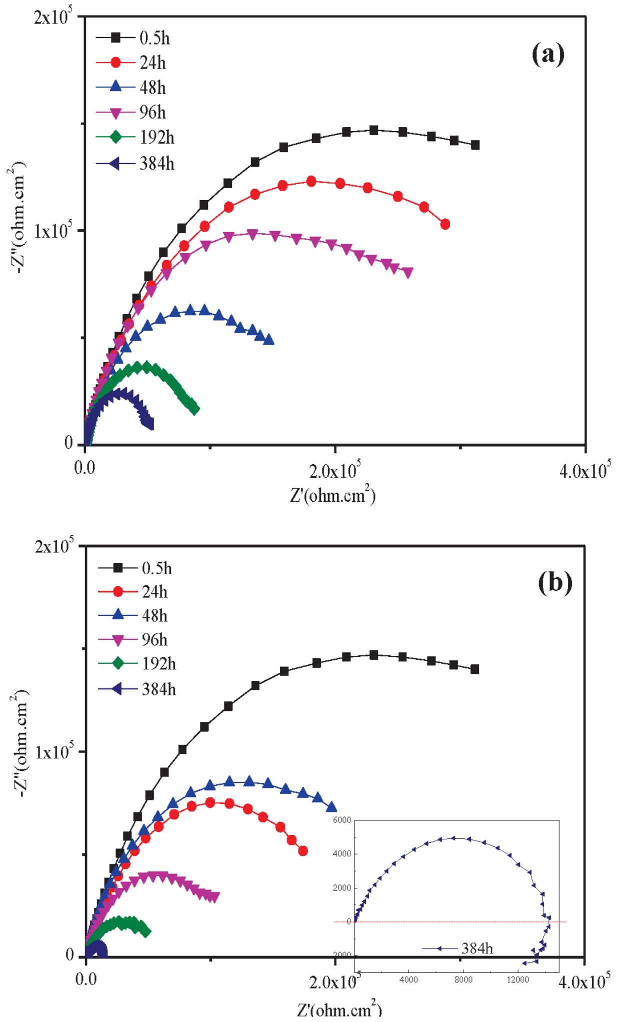

Figure 5: Nyquist plots of PEO-coated aluminum alloy formed in 7 g/L Al_2O_3 containing electrolyte and immersed in solutions for different immersion times: a) 0.5 M NaCl, b) 1M NaCl

3.3.2.2 EIS analysis

To quantitatively analyze the EIS spectra of the coatings in the NaCl aqueous solution, two equivalent circuits were proposed as shown in **Figure 6**. To improve the accuracy of the simulation, the surface inhomogeneity factor and possible diffusional factor were included. A more general constant phase element (CPE)[21], annotated by symbol Q, was used instead of a rigid capacitive element. The capacity element is expressed with the following Equation (1):[22]

$$Z_Q = \frac{1}{Y_0}(j\omega)^{-n} \tag{1}$$

In the Equation (1), j is the imaginary unit ($j^2 = -1$) and ω is the angular frequency ($\omega = 2\pi f$). Coefficient Y_0 or n ($-1 \leq n \leq 1$) is the parameter of the CPE.

In the equivalent circuits presented in **Figure 6**, R_s is the solution resistance between the specimen and reference electrode, R_p is the resistance of the porous layer/coating, paralleled with Q_p (the constant phase element indicating dispersion of the porous coating/layer capacitance) and R_b is the resistance of the inner compact layer paralleled with Q_b. L in **Figure 6b** is the inductance, which is paralleled with R_L. **Figure 6a** was used to fit the EIS data of the coating in diluted 0.5 M NaCl solution up to 384 h and in concentrated 1 M NaCl solution

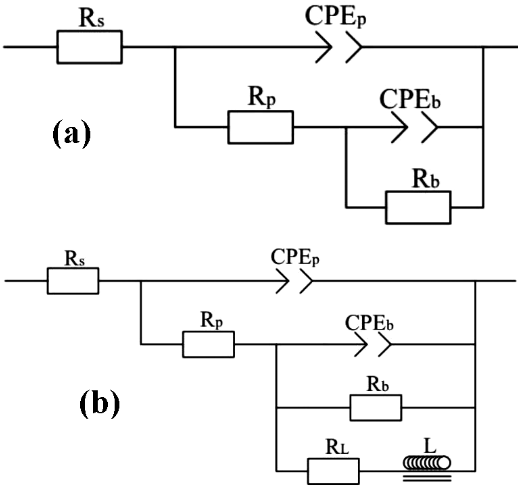

Figure 6: Equivalent circuits for fitting the impedance data for PEO-coated aluminum alloy: a) without inductance, b) with inductance models

Table 1: EIS simulated data of PEO-coated specimen formed in silicate-based electrolytes with 7 g/L Al_2O_3 in 0.5 M NaCl solution after different times of immersion

Immersion time (h)	$R_s/(\Omega\cdot cm^2)$	$R_p/(k\Omega\cdot cm^2)$	$Q_p/(F\cdot cm^{-2})$	n_p	$R_b/(k\Omega\cdot cm^2)$	$Q_b/(F\cdot cm^{-2})$	n_b
0.5	14	27.89	6.82×10^{-6}	0.58	259.87	7.24×10^{-7}	0.74
24	19	19.36	4.52×10^{-6}	0.67	184.52	6.27×10^{-7}	0.85
48	21	12.46	5.68×10^{-5}	0.45	118.64	6.69×10^{-6}	0.81
96	15	17.54	3.57×10^{-5}	0.51	165.3	4.58×10^{-6}	0.92
192	16	9.460	5.39×10^{-5}	0.61	72.16	5.79×10^{-6}	0.70
384	18	7.51	8.64×10^{-5}	0.72	53.24	7.25×10^{-6}	0.69

Table 2: EIS simulated data of PEO-coated specimen formed in silicate-based electrolytes with 7 g/L Al_2O_3 in 1 M NaCl solution after different times of immersion

Immersion time (h)	$R_s/(\Omega\cdot cm^2)$	$R_p/(k\Omega\cdot cm^2)$	$Q_p/(F\cdot cm^{-2})$	n_p	$R_b/(k\Omega\cdot cm^2)$	$Q_b/(F\cdot cm^{-2})$	n_b
0.5	11	26.16	6.46×10^{-6}	0.61	252.17	7.18×10^{-7}	0.83
24	21	14.34	2.86×10^{-6}	0.60	138.92	5.71×10^{-7}	0.79
48	17	15.48	5.67×10^{-5}	0.69	158.96	7.22×10^{-6}	0.84
96	22	10.45	4.29×10^{-5}	0.52	98.76	5.64×10^{-6}	0.69
192	23	5.49	6.52×10^{-5}	0.78	34.78	2.29×10^{-6}	0.88
384	15	2.64	$9.74 \times 1\ 0^{-4}$	0.66	9.21	6.69×10^{-5}	0.71

up to 192 h. **Figure 6b** was used to fit the EIS data of the coating immersed in 1 M NaCl solution for 384 h.

Tables 1 and **2** clearly show that high resistance values of R_p and R_b were registered, i.e., 27.89 kΩ·cm^2 and 259.87 kΩ·cm^2, at the immersion time of 0.5 h in 0.5 M NaCl aqueous solution. Then, with the immersion time increased, the R_p and R_b gradually decreased. Nevertheless, the values of R_p and R_b increased at the immersion time of 96 h, being 17.54 kΩ·cm^2 and 165.3 kΩ·cm^2. After that, R_p and R_b decreased eventually. After 384 h of immersion, R_b dropped to a relatively higher value of 53.24 kΩ·cm^2 compared to the R_p value of 7.51 kΩ·cm^2.

Simulation results exhibited a similar trend in 1 M NaCl aqueous solution. After 384 h of immersion, due to the adsorbed Al^{3+} ions on the surface, inductance occurred. The simulated circuit is changed in **Figure 6b**. The L and R_L are 2.5×10^3 H·cm^{-2} and 310.4 kΩ·cm^2, respectively. These results demonstrate that the coating could not protect the aluminum alloy substrate in 1 M NaCl aqueous solution after 384 h of immersion. The

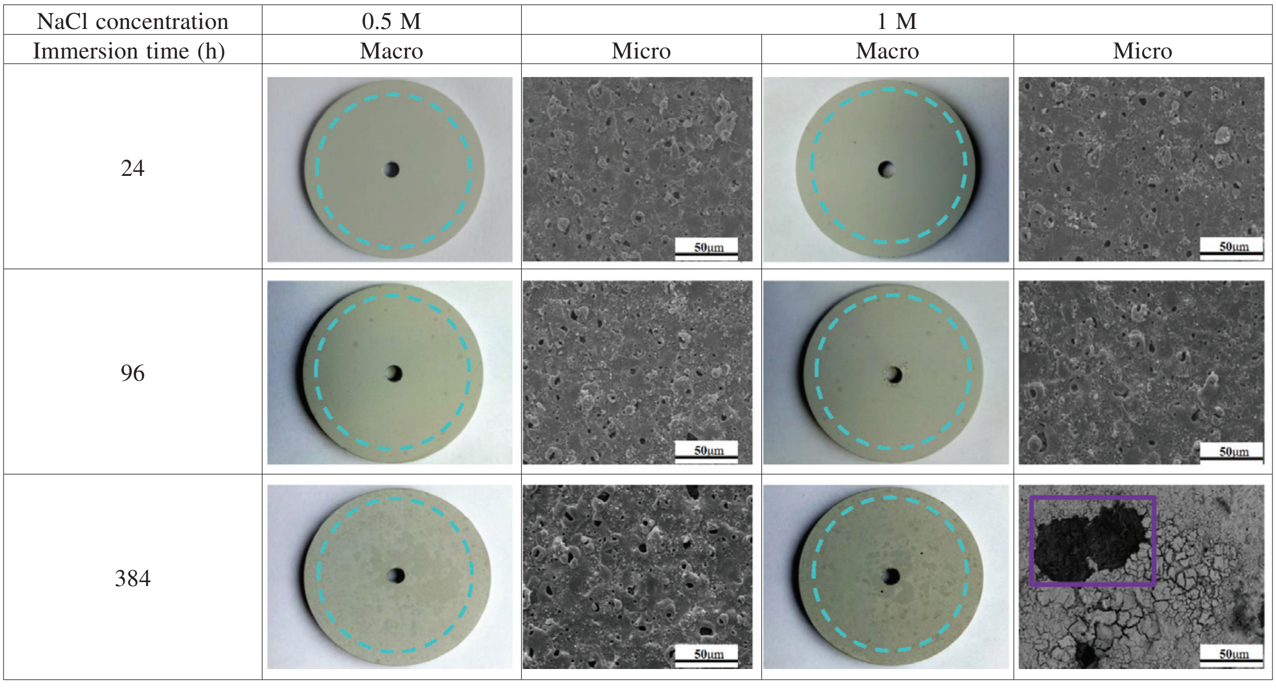

Figure 7: Macroscopic and SEM morphology of corroded surfaces after 24, 96, 384 h of exposure/EIS testing in 0.5 M and 1 M NaCl solution

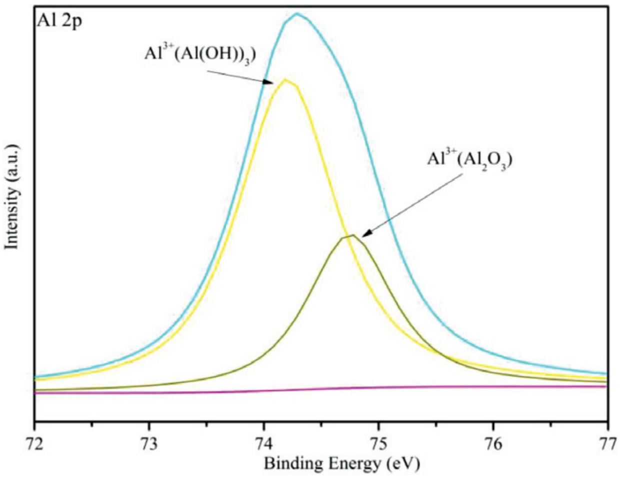

Figure 8: XPS analysis of high-resolution Al 2p spectrum of the PEO coating formed in 7 g/L Al_2O_3 containing electrolyte after the immersion time of 384 h in 1M NaCl solution

variation trend of the EIS results match well with the potentiodynamic polarization results.

3.4 Corrosion morphology of PEO coatings

Macroscopic and SEM morphologies of corroded surfaces after (24, 96 and 384) h exposure/EIS testing in 0.5 M and 1 M NaCl solutions are shown in **Figure 7**. The aqua dash circles marked in macro-morphology show the exposure area (1 cm^2) during the test. In 0.5 M NaCl aqueous solution, there was no evidence of any corrosion damage across the surface of the coating after 384-h EIS testing. However, in 1 M NaCl aqueous solution, the coating was corroded by a gradual Cl^- infiltration. After 384 h of immersion in 1 M NaCl aqueous solution, a large pit (of about 30 µm in diameter) appeared on the surface of the coating. This evidently proved that the aluminum alloy substrate was corroded by the aggressive Cl^- at that time. The corrosion morphology of the coating matches well with the corrosion study above covering the whole immersion process.

3.5 XPS analysis after corrosion

Figure 8 shows the XPS analysis of the high-resolution Al 2p spectrum of the coating formed in 7 g/L Al_2O_3 containing electrolyte after the immersion time of 384 h in 1 M NaCl solution. The purple square in **Figure 7** indicates the analyzed area. From **Figure 8**, it can be seen that the single Al 2p peak at 74.32 eV, typical for Al_2O_3, and unstable corrosion products $Al(OH)_3$ can be decomposed into two peaks at 74.40 eV and 74.20 eV.

3.6. Corrosion mechanism

At the early stage, chloride ion easily penetrates into the pores of the porous layer through discharge channels. Therefore, the corrosion resistance of the coating decreases. Then, with the immersion time prolonged, unstable corrosion products $Al(OH)_3$ can be generated in the pores as shown below:

$$NaCl \rightarrow Na^+ + Cl^- \tag{2}$$

$$H2O \rightarrow H^+ + OH^- \tag{3}$$

$$Al_2O_3 + 6Cl \rightarrow 2AlCl_3 + 3O^{2-} \tag{4}$$

$$H^+ + O^{2-} \rightarrow OH^- \tag{5}$$

$$AlCl_3 + 3(OH)^- \rightarrow Al(OH)_3 + 3Cl^- \tag{6}$$

Then, with the corrosion continued, corrosion products are easily attached to the surface of the coating. To some extent, Cl^- is hard to infiltrate into the coating at this time due to the prevention of corrosion products. So, the corrosion resistance of the coating increases. However, some of the Cl^- can go through the porous layer and react with the barrier layer. Meanwhile, the reaction continues as follows:

$$Al^{3+} + 3H_2O \rightarrow Al(OH)_3 + 3H^+ \tag{7}$$

$$H^+ + Cl \rightarrow HCl \tag{8}$$

Finally, some of the barrier layer is completely corroded. The aggressive Cl^- is in direct contact with the aluminum alloy substrate. The hydrogen evolution reaction occurs as follows:

$$2Al + 6H^+ \rightarrow 2Al^{3+} + 3H^2 \uparrow \tag{9}$$

The coating can no longer provide protection to the aluminum alloy substrate. Thus, the corrosion mechanism discussed above is completely in accord with the corrosion test results.

4 CONCLUSIONS

The objective of this study was to investigate the corrosion of a PEO coating, formed in an electrolyte containing 7 g/L of Al_2O_3, in 0.5 M and 1 M NaCl solutions through electrochemical methods. The summary can be drawn as follows:

1) Long-term potentiodynamic polarization and EIS tests showed that the corrosion resistance of the coating first decreased, then increased and finally decreased.

2) The coating can protect the substrate in 0.5 M NaCl solution after 384-h immersion, but it cannot protect the substrate after 384-h immersion in 1 M NaCl solution.

3) The potentiodynamic polarization results match well with the EIS test results.

Acknowledgments

This work was supported by the open project foundation of High-Tech Key Laboratory of Agricultural Equipment and Intelligence of Jiangsu Province (No. MAET202104), the open foundation of Industrial Perception and Intelligent Manufacturing Equipment Engineering Research Center of Jiangsu Province (No. ZK22-05-07) and the open project foundation of Intelligent Terminal Key Laboratory of Sichuan Province (No. SCITLAB-1013). Dr. Yuanji Shi is indebted to the Qing Lan Project of Jiangsu Province, China, for its financial support.

5 REFERENCES

[1] H. Allachi, F. Chaouket, K. Draoui, Corrosion inhibition of AA6060 aluminium alloy by lanthanide salts in chloride solution, Journal of Alloys and Compounds, 475 (**2009**) 1–2, 300–303, doi:10.1016/j.jallcom.2008.07.017

[2] S. P. Chakraborty, S. Banerjee, I. G. Sharma, P. Bhaskar, A. K. Suri, Studies on the synthesis and characterization of a molybdenum-based alloy, Journal of Alloys and Compounds, 477 (**2009**) 1–2, 256–261, doi:10.1016/j.jallcom.2008.10.093

[3] J. E. Gray, B. Luan, Protective coatings on magnesium and its alloys – a critical review, Journal of Alloys and Compounds, 336 (**2002**) 1–2, 88–113, doi:10.1016/S0925-8388(01)01899-0

[4] A. L. Yerokhin, X. Nie, A. Leyland, A. Matthews, S. J. Dowey, Plasma electrolysis for surface engineering, Surface and Coatings Technology, 122 (**1999**) 2–3, 73–93, doi:10.1016/S0257-8972(99)00441-7

[5] T. S. Lim, H. S. Ryu, S. H. Hong, Electrochemical corrosion properties of CeO_2 containing coatings on AZ31 magnesium alloys prepared by plasma electrolytic oxidation, Corrosion Science, 62 (**2012**), 104–111, doi:10.1016/j.corsci.2012.04.043

[6] H. Fadaee, M. Javidi, Investigation on the corrosion behaviour and microstructure of 2024-T3 Al alloy treated via plasma electrolytic oxidation, Journal of Alloys and Compounds, 604 (**2014**) 15, 36–42, doi:10.1016/j.jallcom.2014.03.127

[7] N. Xiang, R. G. Song, C. Wang, Q. Z. Mao, Y. J. Ge, J. H. Ding, Formation of corrosion resistant plasma electrolytic oxidation coatings on aluminium alloy with addition of sodium tungstate species, Corrosion Engineering, Science and Technology, 51 (**2016**) 2, 146–154, doi:10.1179/1743278215Y.0000000040

[8] X. P. Lu, S. P. Sah, N. Scharnagl, N. Scharnagla, M. Störmer, M. Starykevich, M. Mohedano, C. Blawert, M. L. Zheludkevich, K. U. Kainer, Degradation behavior of PEO coating on AM50 magnesium alloy produced from electrolytes with clay particle addition, Surface and Coatings Technology, 269 (**2015**) 25, 155–169, doi:10.1016/j.surfcoat.2014.11.027

[9] Q. B. Li, J. Liang, Q. Wang, Plasma electrolytic oxidation coatings on lightweight metals, Surface Engineering Treatments, Intech, Rijeka, 2013, 75–99

[10] R. O. Hussein, D. O. Northwood, X. Nie, The effect of processing parameters and substrate composition on the corrosion resistance of plasma electrolytic oxidation (PEO) coated magnesium alloys, Surface and Coatings Technology, 237 (**2013**) 25, 357–368, doi:10.1016/j.surfcoat.2013.09.021

[11] K. R. Shin, Y. S. Kim, H. W. Yang, Y. Gun Ko, D. Hyuk Shin, In vitro biological response to the oxide layer in pure titanium formed at different current densities by plasma electrolytic oxidation, Applied Surface Science, 314 (**2014**) 30, 221–227, doi:10.1016/j.apsusc.2014.06.121

[12] V. Dehnavi, B. L. Luan, D. W. Shoesmith, X. Y. Liu, S. Rohani, Effect of duty cycle and applied current frequency on plasma electrolytic oxidation (PEO) coating growth behavior, Surface and Coatings Technology, 226 (**2013**) 15, 100–107, doi:10.1016/j.surfcoat.2013.03.041

[13] N. Xiang, R. G. Song, J. J. Zhuang, R.-X. Song, X.-Y. Lu, X.-P. Su, Effects of current density on microstructure and properties of plasma electrolytic oxidation ceramic coatings formed on 6063 aluminum alloy, Transactions of Nonferrous Metals Society of China, 26 (**2016**) 3, 806–813, doi:10.1016/S1003-6326(16)64171-7

[14] M. Montazeri, C. Dehghanian, M. Shokouhfar, A. Baradaran, Investigation of the voltage and time effects on the formation of hydroxyapatite containing titania prepared by plasma electrolytic oxidation on Ti-6Al-4V alloy and its corrosion behavior, Applied Surface Science, 257 (**2011**) 16, 7268–7275, doi:10.1016/j.apsusc.2011.03.103

[15] J. J. Zhuang, Y. Q. Guo, N. Xiang, X. Y. Lu, Q. Hu, R. G. Song, Sliding wear behaviour and microstructure of PEO coatings formed on aluminium alloy, Materials Science and Technology, 32 (**2016**) 15, 1559–1566, doi:10.1080/02670836.2015.1132031

[16] Z. J. Wang, L. N. Wu, W. Cai, A. Shan, Z. Jiang, Effects of fluoride on the structure and properties of microarc oxidation coating on aluminium alloy, Journal of Alloys and Compounds, 505 (**2010**) 1, 188–193, doi:10.1016/j.jallcom.2010.06.027

[17] D. Sreekanth, N. Rameshbabu, K. Venkateswarlu, C. Subrahmanyam, L. R. Krishna, K. P. Rao, Effect of K_2TiF_6 and $Na_2B_4O_7$ as electrolyte additives on pore morphology and corrosion properties of plasma electrolytic oxidation coatings on ZM21 magnesium alloy, Surface and Coatings Technology, 222 (**2013**) 15, 31–37, doi:10.1016/j.surfcoat.2013.01.056

[18] P. B. Srinivasan, J. Liang, C. Blawert, W. Dietzel, Dry sliding wear behaviour of magnesium oxide and zirconium oxide plasma electrolytic oxidation coated magnesium alloy, Applied Surface Science, 256 (**2010**) 10, 3265–3273, doi:10.1016/j.apsusc.2009.12.017

[19] S. Aliasghari, P. Skeldon, G. E. Thompson, Plasma electrolytic oxidation of titanium in a phosphate/silicate electrolyte and tribological performance of the coatings, Applied Surface Science, 316 (**2014**) 15, 463–476, doi:10.1016/j.apsusc.2014.08.037

[20] S. Stojadinovic, R. Vasilic, M. Petkovic, B. Kasalica, I. Belča, A. Žekić, Lj. Zeković, Characterization of the plasma electrolytic oxidation of titanium in sodium metasilicate, Applied Surface Science, 265 (**2013**) 15, 226–233, doi:10.1016/j.apsusc.2012.10.183

[21] P. B. Su, X. H. Wu, Y. Guo, Z. Jiang, Effects of cathode current density on structure and corrosion resistance of plasma electrolytic oxidation coatings formed on ZK60 Mg alloy, Journal of Alloys and Compounds, 475 (**2009**) 1–2, 773–777, doi:10.1016/j.jallcom.2008.08.030

[22] P. Zoltowski, On the electrical capacitance of interfaces exhibiting constant phase element behaviour, Journal of Electroanalytical Chemistry, 443 (**1998**) 1, 149–154, doi:10.1016/S0022-0728(97)00490-7